

Learning ride-sourcing drivers' customer-searching behavior: A dynamic discrete choice approach

Junji Urata¹, Zhengtian Xu^{*2}, Jintao Ke³, Yafeng Yin⁴, Guojun Wu⁵, Hai Yang⁶, and Jieping Ye⁷

¹*Department of Civil Engineering, University of Tokyo, Tokyo, Japan*

²*Department of Civil and Environmental Engineering, The George Washington University, Washington DC, Unites States*

³*Department of Logistic and Maritime Studies, The Hong Kong Polytechnic University, Hong Kong, China*

⁴*Department of Civil and Environmental Engineering, University of Michigan, Ann Arbor, United States*

⁵*Data Science Program, Worcester Polytechnic Institute, Worcester, United States*

⁶*Department of Civil and Environmental Engineering, The Hong Kong University of Science and Technology, Hong Kong, China*

⁷*AI Labs, Didi Chuxing, Beijing, China*

May 26, 2022

Abstract

Ride-sourcing drivers spend a significant portion of their service time being idle, during which they can move freely to search for the next customer. Such customer-searching movements, while not being directly controlled by ride-sourcing platforms, impose great impacts on the service efficiency of ride-sourcing systems and thus need to be better understood. To this purpose, we design a dynamic discrete choice framework by modeling drivers' customer search as absorbing Markov decision processes. The model enables us to differentiate three latent search movements of idle drivers, as they either remain motionless, cruise around without a target area, or reposition towards specific destinations. Our calibration takes advantage of large-scale empirical datasets from Didi Chuxing, including the transaction information of five million passenger requests and the trajectories of 32,000 affiliated drivers. The calibration results uncover the variations of drivers' attitudes in customer search across time and space. In general, ride-sourcing drivers do respond actively and positively to the repetitive market variations when idle. They are comparatively more mobile at high-demand hotspots while preferring to stay motionless in areas with long time of waiting being expected. Our results also suggest that drivers' search movements are not confined to local considerations. Instead, idle drivers show a clear tendency of repositioning towards the faraway hotspots, especially during the evening when the demand cools down in the suburb. The discrepancies between full-time and part-time drivers' search behavior are also examined quantitatively.

Keywords: Ride-sourcing service, customer search, driver behavior, dynamic discrete choice

*Corresponding author. E-mail address: zhengtian@gwu.edu (Z. Xu).

1 Introduction

The maturity of mobile internet technology catalyzes on-demand ride-sourcing services provided by companies like Uber, Lyft, and DiDi Chuxing. Compared to traditional street-hailing taxi services, these emerging ride-sourcing services significantly reduce the meeting frictions between riders and drivers, and thus become unprecedentedly popular among urban travelers in recent years (Conway et al., 2018). The great success of ride-sourcing services has attracted a lot of interests on the analysis and management of such on-demand ride-hailing systems (see Wang and Yang, 2019 for a recent review). However, less attention has been paid to the behaviors of ride-sourcing drivers, partially due to the lack of access to service data. To better serve ride-sourcing drivers and facilitate a cohesive platform environment, it is crucial for system managers and policy-makers to understand drivers’ behaviors and concerns in service provision (see, e.g., Sun et al., 2019; Xu et al., 2020). By virtue of comprehensive empirical data from Didi Chuxing, this paper thus aims to comprehend the behavior of ride-sourcing drivers in customer search, which constitutes a significant portion of drivers’ service time and strongly associates with their profitability.

Many empirical studies have been carried out to investigate the customer-searching behavior of taxi drivers, who shares a significant similarity with drivers in ride-sourcing markets. A group of researchers from Hong Kong first applied multinomial logit (MNL) models to capture strategic zonal choices of Hong Kong taxi drivers’ customer search (see, e.g., Wong et al., 2014b, 2015). They proposed a cell-based logit-opportunity model to tackle the local customer-searching behavior of taxis by considering the opportunities along search paths. Recently, Tang et al. (2019) argued that between different destination choices of vacant taxis, there are substantial overlaps in paths, which invalidate the use of MNL models. Instead, they proposed a mixed path size logit-based customer-searching model and tested its effectiveness in predicting routing choices over the trajectory of 36,000 taxis in Beijing. Although these static search models substantially facilitate empirical calibrations, they fall short in capturing the dynamic choice behavior of drivers under the highly varying market conditions. Zheng et al. (2018) modeled vacant taxi drivers’ anticipatory behavior by using a time-dependent framework. However, their study focused on the one-shot decision choices of taxi drivers between urban areas and condensed-demand areas, such as airports and railway stations, and is unsuitable for behavioral calibration. One of the major difficulties in calibrating the search behavior is that drivers’ trajectories do not fully reflect their real preferences. It is common for drivers to get matched to passengers before reaching the actual cruising destinations, especially in app-based ride-hailing markets. Sometimes, drivers do not even have specific search destinations in mind. Therefore, we are in need of a behavioral model that can cope with the intense market variations and identify drivers’ latent search patterns with modeling differentiation.

An alternative way of modeling drivers’ customer-searching movement is to formulate it as Markov decision process (MDP). Oftentimes, an MDP framework is coupled with learning approaches to seek for the optimal searching policy for idle drivers. Recently, Liu et al. (2013), Verma et al. (2017), Gao et al. (2018), and Lin et al. (2018) employed Q-learning to investigate the optimal dynamic routing strategy. This approach does not explicitly characterize the intervening opportunity, but instead implicitly incorporates it into the action rewards through learning. Besides, Qu et al. (2014), Rong et al. (2016), Yu et al. (2020), and Shou et al. (2020) specified structured reward functions based on various zonal features and then solved the problem using dynamic programming. However, the weights of different features were exogenously given to concretize certain search objectives. In general, these learning-based approaches aim at deriv-

81 ing the optimal policy of repositioning drivers for centralized control, and lack the behavioral
82 implications of individual drivers.

83 To fill this research gap, a dynamic discrete choice model is developed in this paper to in-
84 vestigate the customer-searching behavior of ride-sourcing drivers. The model translates market
85 conditions, including both supply and demand information, into a spatiotemporal continuum
86 of opportunity values to idle drivers. Then, by adopting an absorbing MDP framework, we
87 formulate and evaluate drivers’ manifold decisions underlying customer search. To foster a com-
88 prehensive understanding, heterogeneous behavior among different driver types and time of day
89 is further explored and compared. It is worth noting that our model differentiates three modes
90 of search movements, respectively being staying motionless, cruising around without a target
91 area, or repositioning towards a specific destination. These movements, although corresponding
92 to completely different mentality of drivers, are challenging to separate through trajectory data.
93 Indeed, to the best of our knowledge, none of the previous studies has investigated or calibrated
94 the driver behavior in this regard. Leveraging large-scale empirical datasets (with uninterrupted
95 trajectories of 32,000 drivers and transaction information of five million trip requests), this study
96 is dedicated to deepening our understanding of ride-sourcing drivers’ customer-searching be-
97 havior and provide policy insights for the platform’s labor supply management.

98 The remainder of this paper is organized as follows. Section 2 details the dynamic discrete
99 choice model designed for learning ride-sourcing drivers’ customer-searching behavior, while
100 Section 3 illustrates the data preparation for model calibration. Section 4 presents the results of
101 parametric estimation and then interprets the behavioral implications of drivers in zonal search.
102 At the end, Section 5 concludes the paper and points out an future research avenue.

103 **2 Dynamic Discrete Choice Model**

104 This section first introduces the dynamic discrete choice model that we formulate in line with
105 ride-sourcing drivers’ customer-searching movements. We first dissect the process of how idle
106 drivers search for customers, and then formulate a mathematical model to delineate drivers’
107 sequential choice-making. The method for parametric estimation is also discussed.

108 **2.1 Drivers’ customer-searching movements**

109 When ride-sourcing drivers are idle, they enjoy full freedom of deciding where and how to
110 search for the next customer based on the market condition they perceive. They may either
111 remain motionless awaiting the next match, cruise around the neighborhood to actively search
112 for customers, or reposition themselves towards a target hotspot. To cope with these different
113 ways of customer search, we materialize idle drivers’ movements as cyclic decision-making by
114 segmenting them into a series of steps. Within each step, a driver either stays in the current zone,
115 or chooses her next destination from the finite set of adjacent zones and then moves forward. A
116 series of choice decisions are made sequentially by a driver along a chain of connecting zones,
117 until she successfully gets matched with a customer (see Figure 1 for a graphical explanation).

118 For the convenience of behavioral analysis, we further treat the sequential movements as
119 Markov decision processes, assuming that the decision-making of drivers at each step is inde-
120 pendent of her previous choices. Notwithstanding, drivers do plan several steps ahead when
121 making each zonal choice decision. Note that such a setting adheres well with that of the dy-

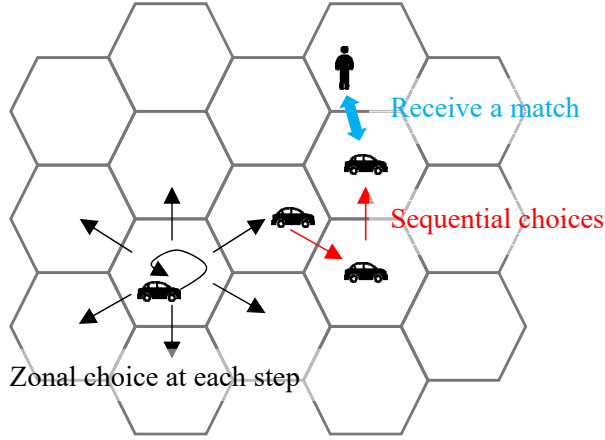


Figure 1: Sequential movements of idle drivers in customer search

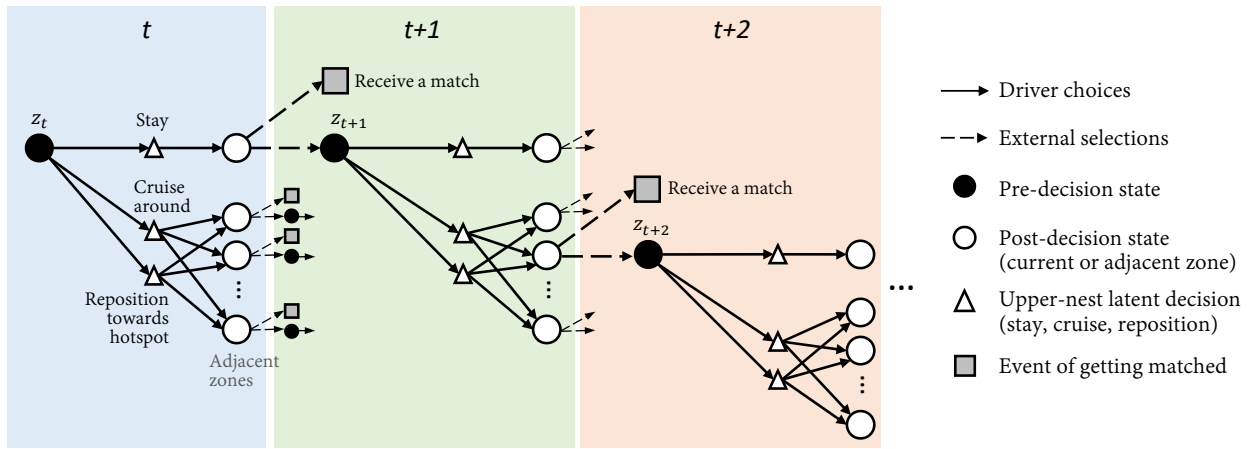


Figure 2: Decision-making processes of ride-sourcing drivers

122 namic discrete choice theory (Rust, 1987). We thus introduce absorbing Markov chains in this
 123 paper to describe the dynamic discrete choices of drivers under finite evaluation horizons.

124 Figure 2 illustrates the cross-nested structure of drivers' sequential searching choices. During
 125 the process, a driver at each stage can select to either rest for a while in the current zone or
 126 move to one of the adjacent zones, based on the expected utility of each choice. The process
 127 continues as the cumulative probability of being matched increases along the trajectory. Within
 128 each stage, the upper nest indicates three latent scenarios for drivers' zonal choices: to either
 129 remain motionless, cruise nearby without a specific destination, or reposition toward a hotspot
 130 area. Correspondingly, the lower nest expands the potential zonal choices under each scenario.
 131 Built on such a cross-nested structure, our model differentiates the latent searching scenarios and
 132 describes drivers' movements more precisely.

133 2.2 Model formulation

134 We formulate the model based on the multinomial-type dynamic discrete choice model proposed
 135 by Rust (1987). Let z_t be the location of a driver at time t . For brevity, we use z_t as an abbreviation
 136 for vector (z_t, t) , which marks the state of an idle driver being at zone z_t at time t . To facilitate
 137 understanding, we first present a base model for non-nested choice cases and then extend it to
 138 more complicated contexts of nested and cross-nested choices. The driver-specific indicators are
 139 omitted in this subsection for clarity.

140 *Base model*

141 With a non-nested choice structure, the expected utility of an idle driver $V^T(z_t)$ at state z_t
 142 under a time horizon of T adheres to the following relationship,

$$143 \quad V^T(z_t) = \mathbb{E} \left[\max_{z_{t+1} \in C(z_t)} \left(v(z_{t+1}|z_t; \theta) + \rho_{z_t} \beta V^T(z_{t+1}) + \epsilon(z_{t+1}) \right) \right]$$

144 where $C(z_t)$ denotes the choice set of drivers at z_t ; ρ_{z_t} is the probability of drivers remaining
 145 unmatched coming through state z_t ; β denotes a time-discounting factor ($0 \leq \beta \leq 1$). Specifically,
 146 on the right side, $v(z_{t+1}|z_t; \theta)$ represents the observed value of an idle driver transitioning from
 147 z_t to z_{t+1} , with θ being a vector of parameters; $\rho_{z_t} \beta V^T(z_{t+1})$ denotes the discounted value of
 148 attaining the state z_{t+1} ; and $\epsilon(z_{t+1})$ entails the error associated with unobserved factors post
 149 state z_{t+1} . Note that ρ_{z_t} in the equation acts similarly as the survival probability in a general
 150 dynamic programming (Rust, 2016). In operations, drivers' customer-searching movements are
 151 forced to termination once they receive matches from the platform. The probability ρ_{z_t} thus
 152 captures the chance that drivers' idleness continues for at least one more periods following z_t . It
 153 is assumed that drivers' customer-searching movements follow utility maximization in each step,
 154 and the values of a driver being matched during the search or reaching the end of a horizon are
 155 both set to zero in the model.

156 Assuming that the error term ϵ follows a Gumbel distribution that has a scaling factor
 157 μ ($\mu \geq 1$) indicating the degree of independence for the unobserved confounders, yields the
 158 following choice probability (with parameter θ omitted for clarity, same below),

$$159 \quad P^T(z_{t+1}|z_t) = \frac{\exp(\mu (v(z_{t+1}|z_t) + \rho_{z_t} \beta V^T(z_{t+1})))}{\sum_{z \in C(z_t)} \exp(\mu (v(z|z_t) + \rho_{z_t} \beta V^T(z)))}, \quad \forall z_{t+1} \in C(z_t)$$

160 where the expected value $V^T(\cdot)$ of each choice can be derived as

$$161 \quad V^T(z_t) = \frac{1}{\mu} \cdot \ln \sum_{z_{t+1} \in C(z_t)} \exp(\mu (v(z_{t+1}|z_t) + \rho_{z_t} \beta V^T(z_{t+1})))$$

162 The choice probability $P^T(z_{t+1}|z_t)$ is then utilized as a surrogate of the state transition probability
 163 from z_t to z_{t+1} , following the same treatment adopted by the recursive logit model (Fosgerau
 164 et al., 2013). It is worth noting that the time horizon T is incorporated to avoid the state explosion
 165 of a time-expanded network amid the varying market conditions. Behaviorally, it could be seen
 166 as the upper bound sensed by drivers for potential search duration. With the horizon T specified
 167 externally, the value of $V^T(z_t)$ can be calculated via backward induction detailed in Section 2.3.

168 *Nested model*

169 As shown by Figure 2, drivers' customer-searching decisions in each step are decomposed as
 170 two levels of nests. They first make an upper-nest decision among stay, cruising, or repositioning,
 171 and then select an adjacent zone out of the lower nest to move one-step forward. Accordingly,
 172 we extend the above base model to accommodate such a context of a nested structure (with no
 173 cross alternatives). The value function under the nested choices is reformulated as follows,

$$174 \quad V^T(z_t) = \mathbb{E} \left[\max_{l \in C_u(z_t)} \left(\epsilon(l) + \max_{z_{t+1} \in C(z_t, l)} \left(v(z_{t+1}|z_t) + \rho_{z_t} \beta V^T(z_{t+1}) + \epsilon(z_{t+1}, l) \right) \right) \right]$$

175 where l is the choice in the upper nest $C_u(\cdot)$. Let $\epsilon(z_{t+1}, l) = \frac{1}{\mu_l} \epsilon(z_{t+1})$ and the error term $\epsilon(z_{t+1})$
 176 follow a standard Gumbel distribution. The value function and inclusive (log-sum) utility v_u are
 177 given by

$$178 \quad V^T(z_t) = \mathbb{E} \left[\max_{l \in C_u(z_t)} \left(\epsilon(l) + v_u(l|z_t) + \epsilon_u(l) \right) \right]$$

$$179 \quad v_u(l|z_t) = \frac{1}{\mu_l} \ln \sum_{z_{t+1} \in C(z_t, l)} \exp \left(\mu_l \left(v(z_{t+1}|z_t) + \rho_{z_t} \beta V^T(z_{t+1}) \right) \right), \quad \forall l \in C_u(z_t)$$

180 Again, assuming $\epsilon(l) + \epsilon_u(l) = \frac{1}{\mu_n} \epsilon(l)$ with $\epsilon(l)$ following a standard Gumbel distribution yields

$$181 \quad V^T(z_t) = \frac{1}{\mu_n} \ln \sum_{l \in C_u(z_t)} \exp(\mu_n v_u(l|z_t)), \quad (\mu_l \geq \mu_n \geq 1) \quad (1)$$

182 and the choice probability exhibits the following multiplicative form,

$$183 \quad P^T(z_{t+1}|z_t) = P^T(z_{t+1}|l) \cdot P^T(l|z_t)$$

$$184 \quad = \frac{\exp(\mu_l (v(z_{t+1}|z_t) + \rho_{z_t} \beta V^T(z_{t+1})))}{\sum_{z \in C(z_t, l)} \exp(\mu_l (v(z|z_t) + \rho_{z_t} \beta V^T(z)))} \cdot \frac{\exp(\mu_n v_u(l|z_t))}{\sum_{k \in C_u(z_t)} \exp(\mu_n v_u(k|z_t))}$$

185 *Cross-nested model*

186 Particularly, in each step, the zonal choices in the lower nest is cross shared by the two upper-
 187 nest intentions, i.e. cruising and repositioning. Further extensions for the cross-nested choices
 188 are obtained through generating functions. In the cases of nested logit (NL) and cross-nested
 189 logit (CNL), the generating functions are respectively given as follows (Train, 2009),

$$190 \quad \text{NL} : G(\mathbf{Y}) = \sum_{l=1}^K \left(\sum_{z \in B_l} Y_z^{\mu_l} \right)^{\frac{1}{\mu_l}}$$

$$191 \quad \text{CNL} : G(\mathbf{Y}) = \sum_{l=1}^K \left(\sum_{z \in B_l} (\alpha_{z,l} Y_z)^{\mu_l} \right)^{\frac{1}{\mu_l}}$$

192 where $\alpha_{z,l}$ is an allocation parameter that reflects the likelihood of alternative z being a member
 193 of nest B_l with $\alpha_{z,l} \geq 0$ and $\sum_l \alpha_{z,l} = 1$; the function Y_z characterizes $\exp(V(z))$ in both models,
 194 where $V(z)$ stands for the value of state z . In comparison, we have $V^T(z_t)$ continue to hold as
 195 Eq. (1) and the log-sum (inclusive) utility v_u under the cross-nested logit be respecified as

$$196 \quad v_u(l|z_t) = \frac{1}{\mu_l} \ln \sum_{z_{t+1} \in C(z_t, l)} \left(\alpha_{z_{t+1}, l} \exp \left(v(z_{t+1}|z_t) + \rho_{z_t} \beta V^T(z_{t+1}) \right) \right)^{\mu_l}, \quad \forall l \in C_u(z_t) \quad (2)$$

197 and the choice probability now sums over all the probability multiplications,

$$\begin{aligned}
 198 \quad P^T(z_{t+1}|z_t) &= \sum_{l \in C_u(z_t)} P^T(z_{t+1}|l) \cdot P^T(l|z_t) & (3) \\
 199 \quad &= \sum_{l \in C_u(z_t)} \frac{(\alpha_{z_{t+1},l} \exp(v(z_{t+1}|z_t) + \rho_{z_t} \beta V^T(z_{t+1})))^{\mu_l}}{\sum_{z \in C(z_t,l)} (\alpha_{z,l} \exp(v(k|z_t) + \rho_{z_t} \beta V^T(k)))^{\mu_l}} \cdot \frac{\exp(\mu_n v_u(l|z_t))}{\sum_{k \in C_u(z_t)} \exp(\mu_n v_u(k|z_t))}
 \end{aligned}$$

200 with $\mu_l \geq \mu_n \geq 1$.

201 2.3 Model estimation

202 All parameters in the model $(\theta, \mu, \beta, \alpha)$, collectively referred to as Θ , can be estimated by maxi-
 203 mizing the following log-likelihood (LL), i.e.,

$$204 \quad \text{LL}(\Theta) = \sum_{i,t} \delta_{i,t}(z_{t+1}|z_t) \cdot \log P^T(z_{t+1}|z_t; \Theta)$$

205 where $\delta_{i,t}$ indicates the choice made by individual driver i at state z_t . The indicator equals to
 206 1 if the driver chose z_{t+1} and 0 otherwise. Note that given all the parameters Θ , the choice
 207 probabilities P^T can be calculated through Eq. (3) using the expected utilities V^T , which is
 208 treated as fixed via backward induction. As per the recursive Eqs. (1) and (2), the utilities V^T
 209 of preceding states at time t can be computed based on the succeeding states' at $t + 1$. Since the
 210 terminating state value at the end of each horizon is prespecified as 0, we can thus recursively
 211 calculate the utility of all the states. The estimation of Θ can be carried out in a similar fashion as
 212 that for the network Generalized Extreme Value models (Daly and Bierlaire, 2006). The Student's
 213 t -tests are conducted to examine the significance of parametric estimates in the model, while
 214 Watson and Westin pooling tests are applied for model comparisons (Watson and Westin, 1975).

215 3 Data Description

216 Two datasets from Didi Chuxing are used for model calibration. One records the trajectory
 217 information of drivers while the other contains the complete transaction information of trip
 218 requests from one medium-sized city in China, spanning over the 10 weekdays in August 7-18,
 219 2017.

220 The trajectory data comprises the spatiotemporal records of 32,000 DiDi drivers. Each tra-
 221 jectory characterizes a series of status points of a particular driver recorded every 3 seconds
 222 throughout a nonstop customer-searching segment; and each status point consists of a times-
 223 tamp, longitude and latitude coordinates of a driver, as well as her service state at that moment,
 224 either being idle (waiting to be matched), deadheading (picking up a customer), or occupied
 225 (delivering a customer to the destinations). The entire city is partitioned into regular hexagonal
 226 lattices, each being side-connected with six adjacent ones. The major advantage for hexago-
 227 nal partition is that each unit has six symmetrically equivalent and unambiguous side-adjacent
 228 neighbors, while square partition results in two different types of neighboring, respectively be-
 229 ing side-connected or corner-connected. We map the latitude/longitude sequences to the 660-
 230 meter-side-length hexagonal lattices (Sahr et al., 2003) to produce the base sample for movement
 231 identification. Overall, the searching distances of idle drivers were not overwhelming in this

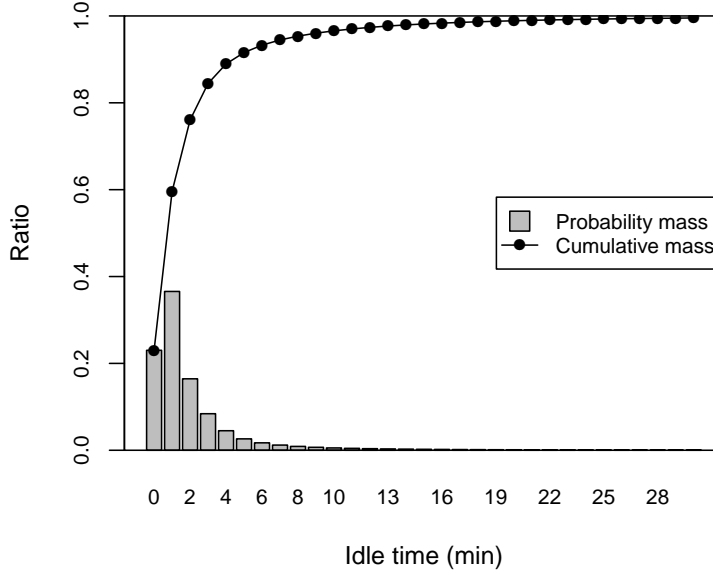
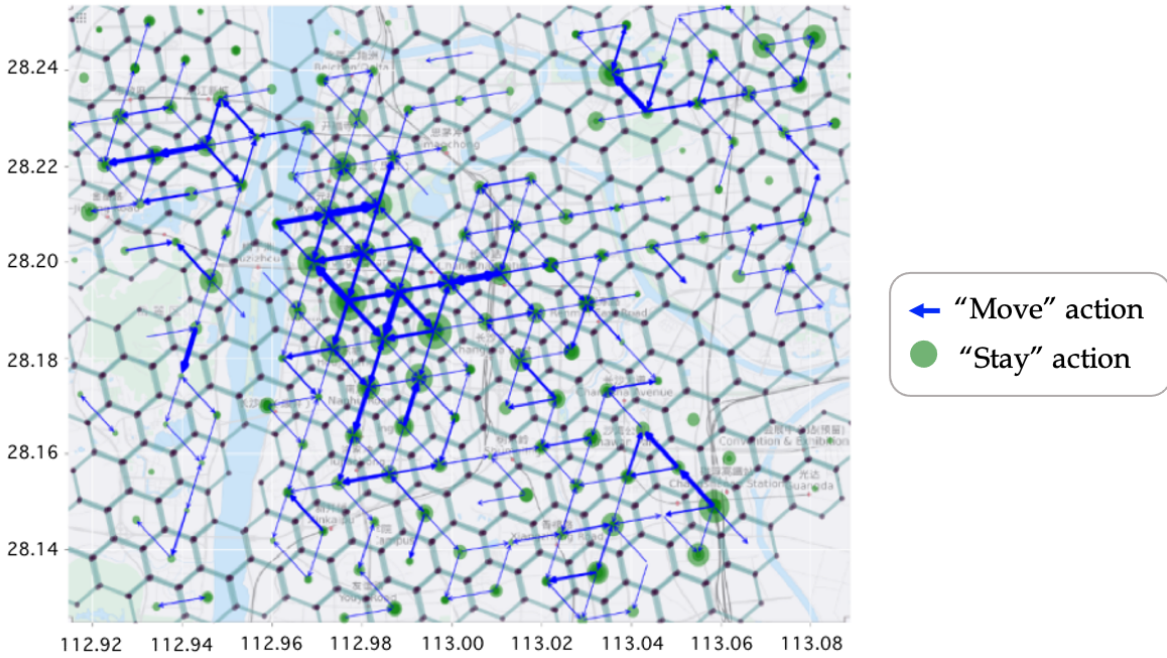


Figure 3: Histogram of drivers' idle time staying in one zone

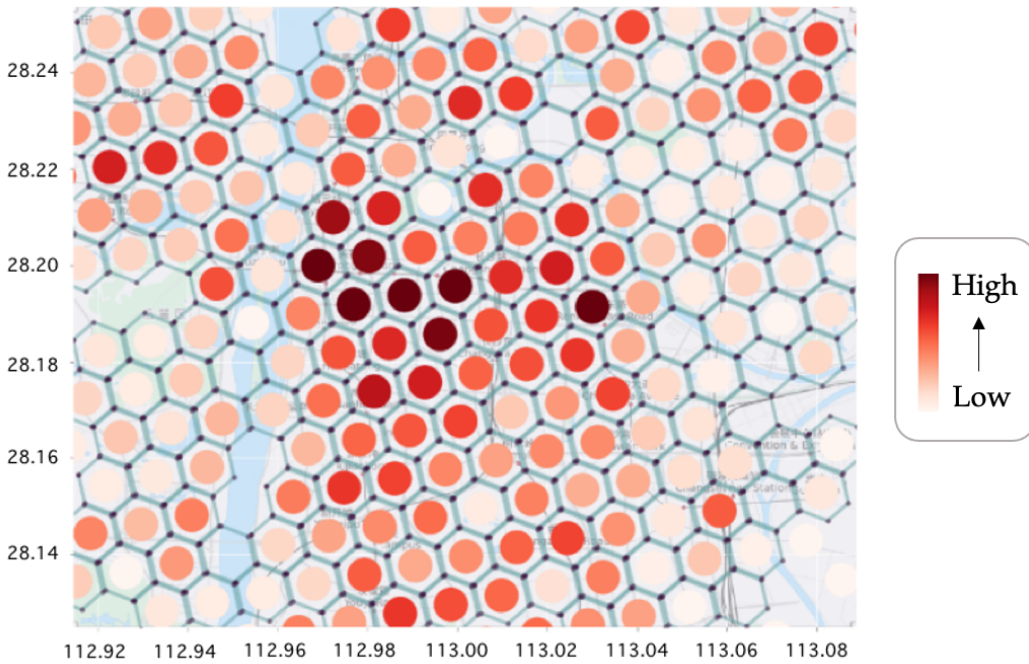
city. Above 80% of the trajectories in the dataset cover no more than 3 zones. The case when an idle driver remains in one specific zone for a duration exceeding a threshold κ is regarded as a “stay”, while the case that a driver repositions to a neighboring zone within κ is taken as a “move”. Those searching trajectories with a total duration less than κ are removed from our sample. Figure 3 plots the distribution of drivers' consecutive idle time of staying at one single zone. We finalize the selection of κ to be four minutes to buffer the time needed by divers to wait for traffic signals and pass through zones.

The transaction dataset contains the information of approximately five million request records. Each record comprises the timestamp when the trip gets requested, the origin/destination of the trip, the matching/pickup/delivery time of the passenger, the driver in service, and the trip fare. The transaction information is aggregated by hexagonal zones and time of day to produce various covariates associated with the market conditions. It is worth noting that to overcome the sparsity of data under the high-granularity partition, this study does not differentiate between days. All the records fall in the same time interval across different days are merged together to create the within-day explanatory variables. Consequently, the coefficient estimation results likely reflect drivers' behavior in response to the regular market variations from day to day rather than the transient and random fluctuations.

As an overview of the datasets, Figures 4a and 4b visualize the spatial distributions of drivers' movements and the number of orders being requested, respectively. In Figure 4a, the blue arrow represents the number of samples moving between two adjacent zones (“move” action), while the green circle refers to the number of samples staying in the current zone (“stay” action). Figure 4b shows the heat map of the number of orders averaged over all the five-minute intervals for each hexagonal zone. It can be observed that the variations of supply and demand are highly consistent in space. Figure 5 displays a boxplot for ratio ρ_{z_t} that idle drivers remain unmatched in each 12-min interval of a day. As clearly shown by the figure, the matching probability of drivers changes drastically throughout a day. Following the searching processes detailed in Section 2, this essentially implies the time-varying range and composition of drivers' zonal choices, thereby



(a) Drivers' movements



(b) Order requests

Figure 4: Spatial distributions of a) drivers' search trajectories and b) orders requested. The blue arrows and the green circles in the top figure represent the number of "move" and "stay" actions, with thicker arrows and larger circles standing for higher counts, respectively. The heatmap at the bottom illustrates the contrasts of ride requests over the space, with deeper colors representing higher service demand.

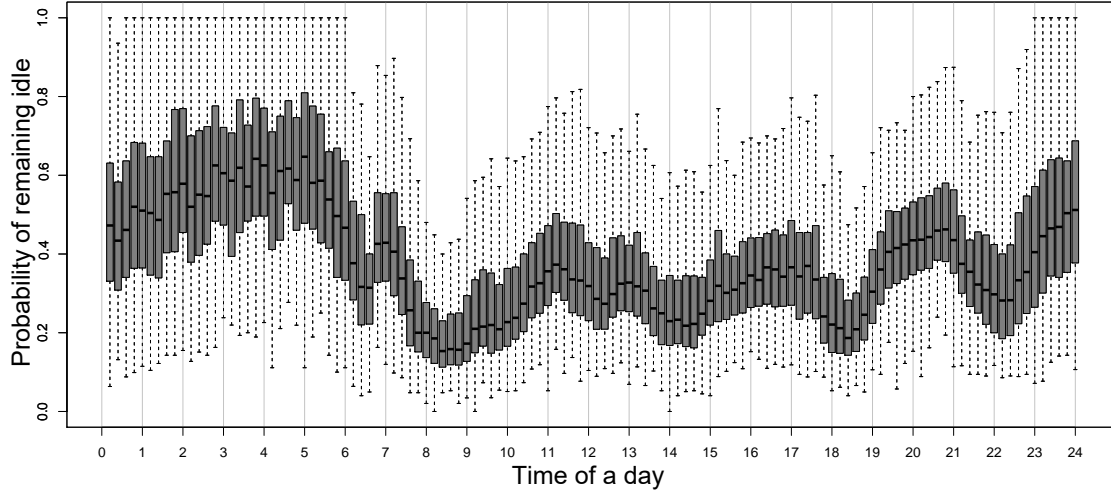


Figure 5: Probability of idle drivers remaining unmatched in each 12-min interval of a day. The bold line traces the median ratios across all the zones within each interval, while the dark gray boxes and the dotted segments display the [25th, 75th] and the [5th, 95th] percentile ranges, respectively.

259 questing the need for a dynamic model to delineate the choice-making.

260 In addition, depending on their service patterns, drivers considered in this study are di-
 261 vided into two classes, respectively as full-time and part-time drivers. Full-time drivers are those
 262 with the most extended service hours but also the highest earners and most profitable ones.
 263 They are mostly daytime workers and display very little within-group heterogeneity in terms of
 264 profitability. In contrast, part-time drivers are active for less amount of time and show signif-
 265 icant within-group disparities in driving and working experiences, as well as profitability and
 266 earnings.

267 4 Model Estimation and Behavioral Interpretation

268 A set of explanatory variables are generated from the above datasets and then fed into the dy-
 269 namic discrete choice model for parametric estimation. In this section, we base on the coefficient
 270 estimates to interpret drivers' factorial focuses underlying the customer-searching movements.

271 4.1 Parametric setup

272 The following explanatory variables are generated to represent the variable market condition:

- 273 • Trip fare TF_z^t : The average trip fare of orders originated in zone z during time interval t ;
- 274 • Number of requests NR_z^t : The total number of requests sent out in zone z during time
 275 interval t ;
- 276 • Pickup time PT_z^t : The average pickup time of passengers requesting for trips in zone z
 277 during time interval t ;

- Matching probability MP_z^t : The ratio of idle drivers receiving matches in zone z during time interval t .

To be consistent with the movement threshold κ , the time granularity for the four market variables are set as 4 minutes. The first three variables are further normalized to distributions with zero mean and unit standard deviation. It is also verified that the partial correlation among the explanatory variables is fairly low, and collinearity should not be a concern here. All these variables are then invited to construct the observed utility $v(z_{t+1}|z_t)$ in Eq. (2) as follows¹,

$$v(z_{t+1}|z_t, \theta) = \theta_{TF}TF_{z_{t+1}}^t + \theta_{NR}NR_{z_{t+1}}^t + \theta_{PT}PT_{z_{t+1}}^t + \theta_{MP}MP_{z_{t+1}}^t + \theta_{SZ}\mathbb{1}(z_{t+1} = z_t)$$

where coefficient θ represents drivers' sensitivity to different factors. Specifically, θ_{SZ} is a movement constant that indicates drivers' preference for remaining motionless when idle; $\mathbb{1}(\cdot)$ characterizes an indication function that values 1 when the condition within the bracket holds and 0 otherwise.

To better capture the strategic movements of idle drivers, we introduce another variable—distance to the hotspot DH_z^h —that calculates the Euclidean distance from the centroid of zone z , where the driver stays, to that of the hotspot h . The hotspot areas are carefully selected in each of the five periods of a day, i.e. morning (6AM-10AM), daytime (10AM-4PM), evening (4PM-8PM), night (8PM-11PM), and midnight (11PM-6AM). For each zone, we sum up the number of requests by 20-min intervals and then calculate the 80th-percentile and the maximum counts in each separate period. A zone is then identified as a hotspot in the period if the 80th-percentile count falls below the maximum by less than 10 percent. The selected hotspots are mostly downtown areas, commercial areas in the suburb, and railway stations, which are further categorized into the downtown-hotspot area (DTH) and the outer-hotspot area (OUH). Our cross-nested logit model treats these two hotspot categories separately in the upper nest, and the variable DH_z^h calculates the distance to the closest hotspot in each category. The allocation parameter $\alpha_{z_t,l}$ in Eq. (3) are specified as follows:

$$\begin{aligned} \alpha_{z_t,h} &= \frac{\exp(\gamma_{DH}DH_{z_t}^h)}{S}, \quad \forall h \in \{DTH, OUH\} \\ \alpha_{z_t,c} &= \frac{\exp(\gamma_{NR}NR_{z_t}^t)}{S} \\ S &= \exp(\gamma_{DH}DH_{z_t}^{DTH}) + \exp(\gamma_{DH}DH_{z_t}^{OUH}) + \exp(\gamma_{NR}NR_{z_t}^t) \end{aligned}$$

where $\alpha_{z_t,h}$ and $\alpha_{z_t,c}$ denote the weights for the target-specific repositioning and aimless-cruising movements, respectively; the coefficients γ represent a set of parameters that indicate drivers' sensitivity to the factors in different searching categories. We note that the factor specifications for allocation parameters above are refined through stepwise selections from a list of variables.

The choice set of drivers $C(z_t)$ at each state is extracted from the observations, and the scaling factor μ_n is set to 1. Meanwhile, the sample is split evenly into two for the purpose of learning and validation. We employ the Nelder–Mead method, one of the best-known algorithms for derivative-free optimization of unconstrained problems, to estimate the parameters.

¹Note that many other factors, such as drivers' home location, parking availability, and traffic congestion etc., may dictate drivers' customer-search movements but are omitted in this study due to our data limitation. Once available, they are advised to be incorporated to reduce the potential omitted variable bias in result interpretation.

Table 1: Model comparisons for different evaluation horizons T

Horizon T (step)	0 (static)	1	2	3	4	5
LL	-112,311	-112,235	-112,221	-112,220	-112,220	-112,220
LL (validation)	-109,803	-109,743	-109,726	-109,724	-109,724	-109,724

Table 2: Model comparisons for juxtaposed nest structures and granularities of ρ_{z_t}

Nest structure ρ_{z_t} 's updating frequency	Cross-nested			Nested	Plain
	4 min	2 h	Never	4 min	4 min
LL	-112,221	-112,266	-112,261	-112,253	-112,875
LL (validation)	-109,726	-109,758	-109,755	-109,761	-110,440

314 4.2 Model refinement

315 With the value functions specified, we then refine the selection of critical parameters and struc-
 316 tures in the model, i.e., the horizon of evaluation T , the updating frequency of the probability
 317 ρ_{z_t} , and the nest structure.

318 Table 1 compares the models under a set of different evaluation horizons T , based on the
 319 sample of full-time drivers. As shown in the table, the LLs in validation follow the same trend as
 320 that from model estimations, relieving the concerns for overfitting. The LL for the model when
 321 $T = 0$ (a static model) appears the lowest, implying the relative superiority of our proposed
 322 dynamic choice model. Besides, the LL increases constantly as T grows from 0 to 2, and stays
 323 constant afterwards. Considering the computational efficiency, we adopt $T = 2$ in the final
 324 implementation to account for the ahead-planning behavior of drivers in customer search.

325 Table 2 compares the models with different updating frequencies of ρ_{z_t} and juxtaposed nest
 326 structures. First, for the cross-nested case, we present three models where ρ_{z_t} gets updated
 327 every 4 minutes, 2 hours, and never (by fixing ρ_{z_t} to 1), respectively. According to the LLs, the
 328 model with the most frequently updated ρ_{z_t} works the best. Then, we zoom out to compare
 329 the modeling effectiveness of different nest structures. The nested logit model keeps only the
 330 stay/leave options in the upper nest (therefore, with no crossings in the zonal alternatives), while
 331 the plain structure practices the most basic logit model. The utility specifications of both models
 332 include the hotspot variables DH_z^h by linear combinations. Not surprisingly, the cross-nested
 333 model outperforms the other two and is thus selected for our later analyses.

334 4.3 Full-time versus part-time drivers

335 Based on the cross-nested model, we apply the pooling test by Watson and Westin (1975) to ex-
 336 amine whether full-time and part-time drivers in general behave differently in customer search.
 337 The restricted model applies a unified set of coefficients for both types of drivers, while the alter-
 338 native model specifies two separate sets of coefficients. The likelihood-ratio (LR) test statistic is
 339 significant at the 1% level, which confirms the heterogeneous searching behavior among different
 340 types of drivers. The specific parametric estimation as well as the significance of each estimate
 341 are presented in Table 3. The left two sets of columns respectively summarize the estimates of
 342 Θ for full-time and part-time drivers, while the right two columns present the two classes of
 343 drivers' comparative differences $\Delta\Theta$ in response to the various factors.

Table 3: Coefficient estimates of a cross-nested model with two types of drivers

Param. Est.	Full-time $\hat{\Theta}$		Part-time $\hat{\Theta}$		Difference $\Delta\hat{\Theta}$	
	Coef.	<i>t</i> -Stat.	Coef.	<i>t</i> -Stat.	Coef.	<i>t</i> -Stat.
<i>Utility parameter</i>						
θ_{TF}	0.02	2.40 [†]	0.05	3.83*	0.03	1.77
θ_{NR}	0.08	37.02*	0.06	21.40*	-0.01	-3.77*
θ_{PT}	-0.02	-3.11*	0.08	7.91*	0.10	8.27*
θ_{MP}	1.00	18.29*	0.60	8.00*	-0.40	-4.30*
θ_{SZ}	1.70	199.62*	1.78	135.86*	0.09	5.45*
<i>Allocation parameter</i>						
γ_{DH}	-3.68	-8.00*	-3.17	-6.25*	0.51	0.74
γ_{NR}	0.52	8.46*	0.45	6.13*	-0.07	-0.78
Discount β	0.31	23.08*	0.17	7.46*	-0.14	-5.30*
Scaling μ_l	1.74	68.90*	1.91	39.22*	0.17	3.16*
Observations	166,171		83,778		249,188	
LL(0)	-184,763		-93,047		-277,810	
Final LL	-112,221		-53,042		-165,264	
LL (validation)	-109,726		-52,217		-161,942	
Adjusted ρ^2	0.39		0.43		0.41	

Notes: The left two sets of columns show the coefficient estimates respectively for full-time and part-time drivers, while the rightmost two columns present the differences in drivers' response between the two classes of drivers (i.e. the part-time drivers' minus the full-time drivers' counterparts). The former results are estimated using separate datasets corresponding to each driver type, while the latter uses the full set of data.

† - Significance to the 5% level;

* - Significance to the 1% level.

344 As shown by Table 3, most of the coefficient estimates $\hat{\Theta}$ are significant at the 1% level for
345 both full-time and part-time drivers, with intuition-consistent signs. This implies an encourag-
346 ing fact that in general ride-sourcing drivers do respond actively and positively to the repetitive
347 market variations. The only counter-intuitive result is that $\hat{\theta}_{PT}$ is positive for part-time drivers.
348 It means that part-time drivers tend to drive to the area with longer pickup time for passengers.
349 In fact, different from the rest explanatory variables, the metric of passengers' pickup time PT_z^t
350 is obscure to drivers, and the estimate $\hat{\theta}_{PT}$ may embody drivers' response to other market factors
351 in relevant. For instance, the negative $\hat{\theta}_{PT}$ of full-time drivers may partially reflect their aversion
352 to the congested areas in zonal choice, while the counter-intuitively positive $\hat{\theta}_{PT}$ for part-time
353 drivers could be that they prefer the areas where they can match to customers in a wider space
354 (higher matching opportunity but longer pickup time), or the areas with more condensed cus-
355 tomer demand but also more congestion in usual. Besides, as revealed specifically by our model,
356 drivers' searching movements are not confined to the local considerations. Instead, they show
357 a clear tendency of repositioning towards the faraway hotspots, which strengthens significantly
358 as they move closer to those areas. It is highly probable that drivers take the distant hotspots as
359 back-up options given the certainty of receiving quick matches therein, similar to the inclination
360 of taxi drivers for taxi stands outside the city center (Szeto et al., 2019). But as a result, all the
361 supply of idle drivers at the neighborhood of a hotspot might be drained up, causing deceptive
362 supply shortage in local regions.

363 While drivers of different groups hold consistent preferences for the various factors in cus-
 364 tomer search, there is a significant disparity between full-time and part-time drivers in response
 365 sensitivity. In contrast to full-time drivers, drivers work in part-time are much less sensitive to
 366 the number of requests and the matching probability in zonal search. This is consistent with
 367 our intuition that full-time drivers are more experienced in service provision and can thus re-
 368 spond scrupulously under different circumstances. Interestingly, part-time drivers characterize
 369 a significantly lower discount factor β compared to full-time drivers. In accordance with the
 370 role of β as a time-discounting factor, this implies that full-time drivers are more far-sighted by
 371 planning ahead, while part-time drivers focus more on the near-future opportunities. Mean-
 372 while, the scaling parameter μ_l for full-time drivers is significantly lower, meaning that their

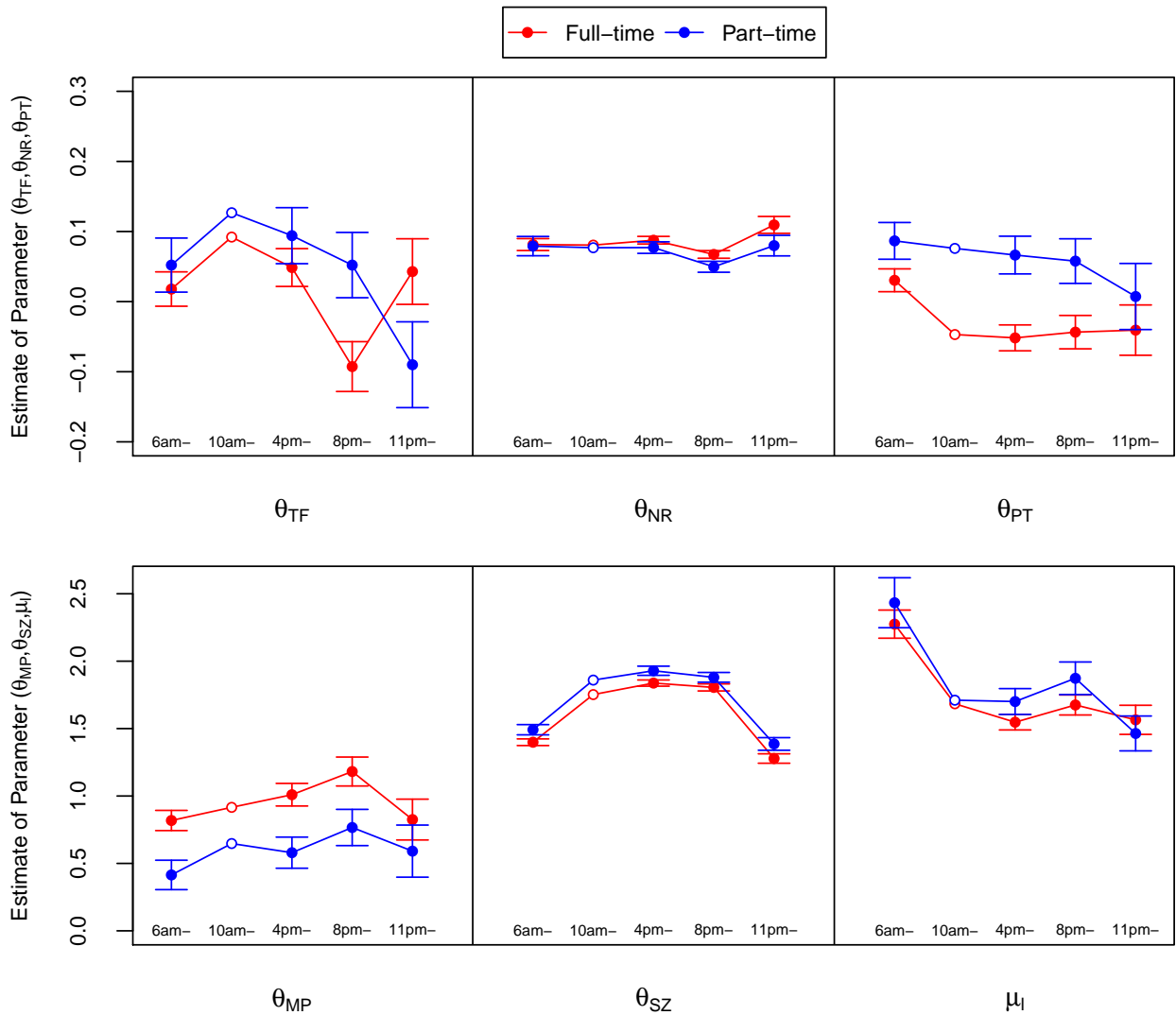


Figure 6: Comparisons of drivers' behavioral responses across the time of a day. On each parameter, the estimate $\hat{\Theta}$ corresponding to the daytime period (10:00 AM-4:00 PM) is set as the baseline, while the relative deviations $\Delta\hat{\Theta}$ of the other time periods are tested. The dots present the absolute value of estimates $\hat{\Theta}$ across different periods, while the error bars around indicate the standard deviations for $\Delta\hat{\Theta}$.

373 customer-searching movements are dictated more strongly by unobserved confounders.

374 We then proceed to examine whether drivers’ searching behavior varies in time by allowing
375 the coefficients to change by periods of time. To ensure the validity of calibration over the seg-
376 mented datasets, we fix the discounting factor β and allocation factor γ in each sub-model to the
377 value estimated previously using the full sample. Figure 6 displays the parametric estimates of
378 full-time and part-time drivers across the time of a day, respectively. According to the figure, the
379 two classes of drivers again exhibit very similar temporal patterns in response to the various fac-
380 tors. They both show higher preference on the trip fare during the daytime, while focusing more
381 on the matching probability in the evening. Such a behavioral transition adheres with the nature
382 of ride-sourcing markets, as the travel demand becomes much more sparse and heterogeneous
383 spatially after the evening peak, when drivers need to switch searching goals to first secure the
384 chances of getting matched. Meanwhile, the estimates of the movement coefficient θ_{SZ} indicate
385 that drivers prefer to stay motionless in the afternoon and evening (specifically, from 10:00 AM
386 to 11:00 PM), while moving more actively at late night and early morning. This contrast partially
387 results from the fact that many drivers start their shifts before the morning peak and end at late
388 night. During those periods, the searching behavior of drivers can be vastly influenced by their
389 inclination to either reposition towards ideal service areas or move back home.

390 4.4 Space-time-dependent preference of searching movements

391 Applying the calibrated model above, we then derive the choice probabilities of full-time drivers
392 at different locations and periods to further investigate how their latent behavior adapts to the
393 variable market conditions. We note that full-time drivers constitute the majority of labor supply
394 in the ride-sourcing service, characterizing a group comparable to the traditional taxi drivers. To
395 yield comparable choice probabilities across time, we drop the outer-hotspot choices from the
396 upper nest across the periods and then estimate the coefficients using models with a consistent
397 upper nest.

398 Figure 7 and 8 visualize the zonal choice probabilities of full-time drivers at different areas
399 in two typical periods to highlight the difference of drivers’ latent searching movements between
400 daytime and nighttime. Figure 7 first presents the probabilities for drivers in each zone to repo-
401 sition to the downtown hotspot when being idle, with larger and darker pies marking the higher
402 probabilities (same for the figures presented later in this section). As can be seen clearly, idle
403 drivers, except for those at the few zones on the outskirts of the city, prefer less the choice of repo-
404 sitioning to the downtown hotspot during the daytime. In contrast, as the suburban market cools
405 down significantly during the evening, idle drivers show much stronger willingness to reposition
406 and escape the potentially long time of wait therein. Such insights are also suggested by Figure
407 8, which details the contrasts by visualizing the stepwise choice probabilities over the space.
408 Each arrow denotes the choice of moving from the origin zone towards a neighboring zone, and
409 again darker color indicates that the corresponding movement is chosen with a higher probability
410 among all the choices available at the origin. Connecting all these preferences pictures the move-
411 ment tendency of idle drivers within the spatial market. It can be easily observed that compared
412 to the daytime (Figure 8a,b), idle drivers during the nighttime show much higher preferences
413 for moving rather than staying motionless (Figure 8c,d). Meanwhile, the upward(downward)
414 arrows in the south(north) side carry darker colors, which essentially implies the inclination of
415 idle drivers moving to the central area to receive matches more easily. The pattern of drivers
416 gathering from the suburban areas to the downtown is greatly strengthened at night. Similar
417 behaviors were also observed and reported by Wong et al. (2014a, 2015) for taxi drivers in Hong

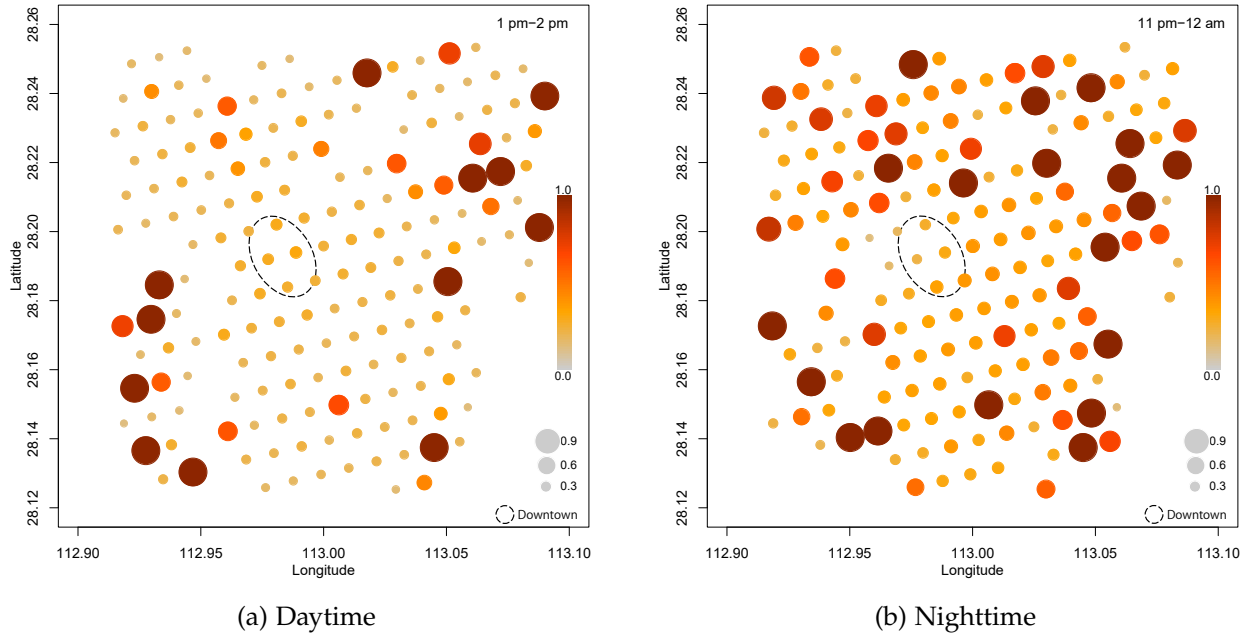
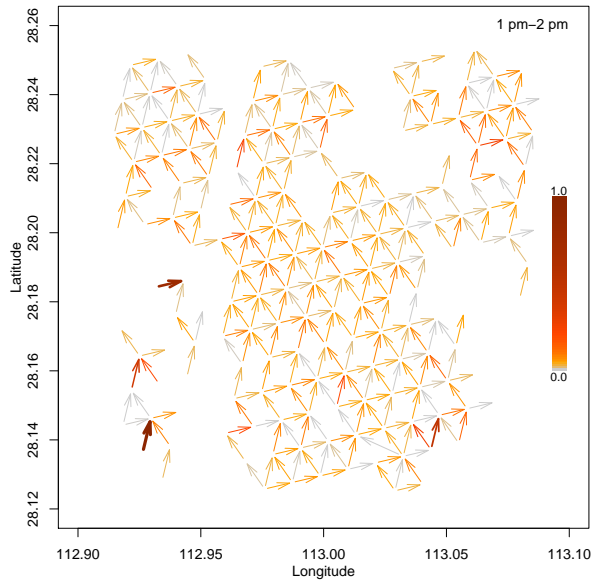


Figure 7: Choice probability of idle drivers repositioning towards the downtown in each zone, with larger and darker pies representing the higher probabilities. The dotted circles in the center mark the downtown area of the city.

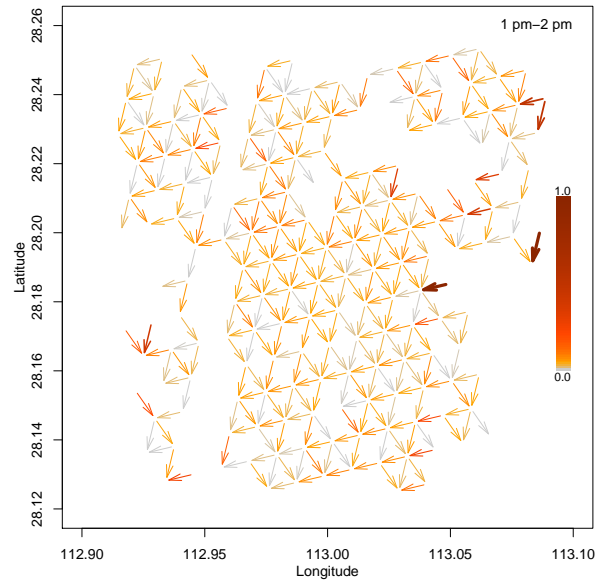
418 Kong.

419 Figure 9 and 10 display the choice probabilities of full-time drivers for staying motionless
 420 and cruising around the neighborhood, respectively, at four representative periods of a day.
 421 Interestingly, we find that drivers are consistently more mobile in the central areas compared
 422 to the suburbs. At those regions with rarer travel demand, ride-sourcing drivers prefer to stay
 423 motionless rather than moving and searching for customers, which somehow differs from that
 424 of taxi drivers. As per Wong et al. (2014a), taxi drivers do not show a clear preference for
 425 traveling towards taxi stands and waiting there for customers at the low-demand areas. In fact,
 426 we suspect that such an attitudinal difference between ride-sourcing and taxi drivers might be
 427 due to the nature of search frictions under the two ride-hailing modes. Taxi drivers mainly serve
 428 customers waving on the curbside and can thus improve their service efficiency substantially
 429 through local hunting (Zhang et al., 2014). In contrast, the app-based e-hailing services eliminate
 430 the physical barriers between drivers and passengers in matching, under which zonal search of
 431 drivers does not necessarily increase the chances of being matched but pushes up the operational
 432 costs, especially in places with sparse trip demand.

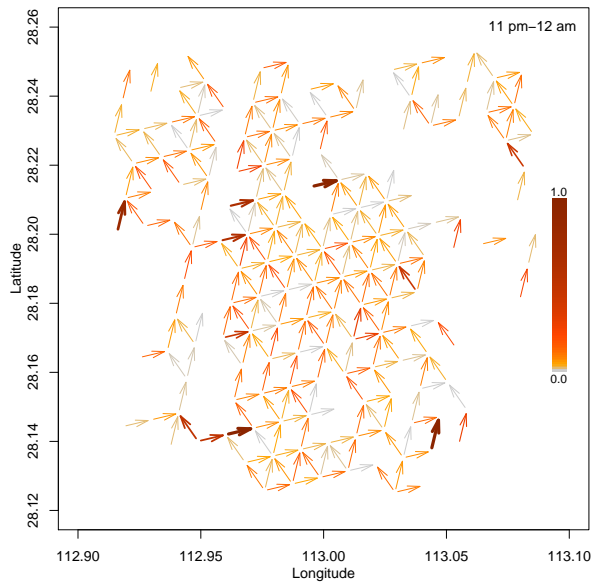
433 The temporal variations of choice probabilities are also intriguing. For example, the cruising
 434 behavior of drivers appears weakly in a wide range of areas during the morning peak (Figure
 435 10a), and then almost disappears afterward (Figure 10b). Later, starting from the evening peak,
 436 while the cruising effect remains weak in the suburbs, it rebounds in the downtown as well
 437 as around the railway station (at the southeast corner) and intensifies in the evening up until
 438 midnight. Such a trend agrees well with those of taxi drivers, who are reported to be more
 439 willing to circulate within local regions during the morning peak but prefer to wait motionlessly
 440 for customers at the evening peak (Wong et al., 2015). Again, such time-varying behavior of
 441 drivers could also be a result of their strategic reaction to the changeable contrasts between



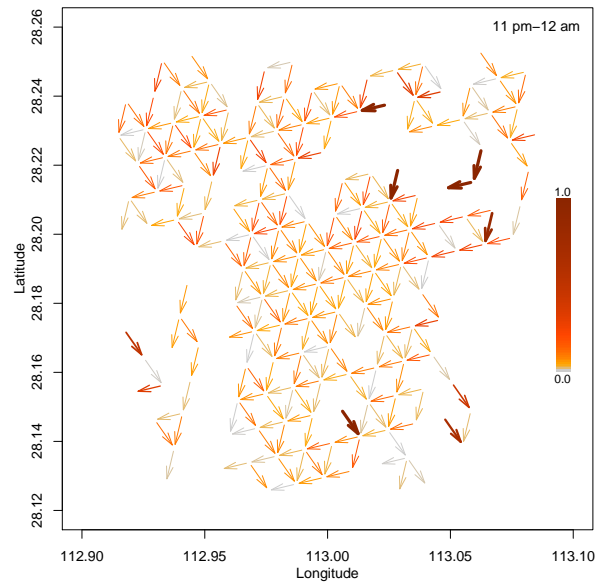
(a) Daytime, Upwards



(b) Daytime, Downwards

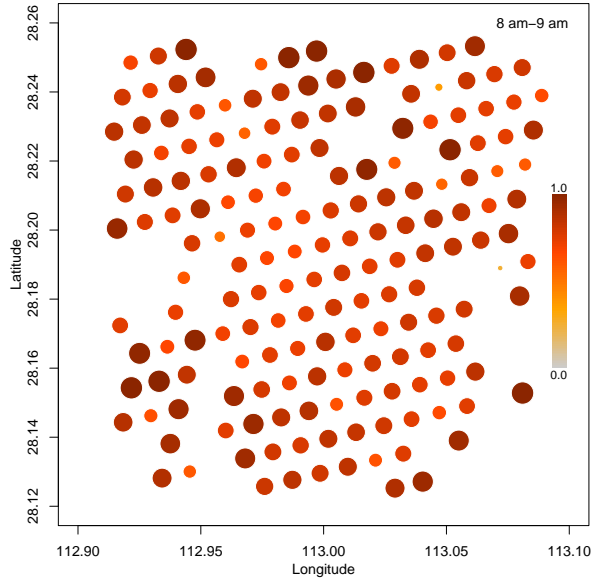


(c) Nighttime, Upwards

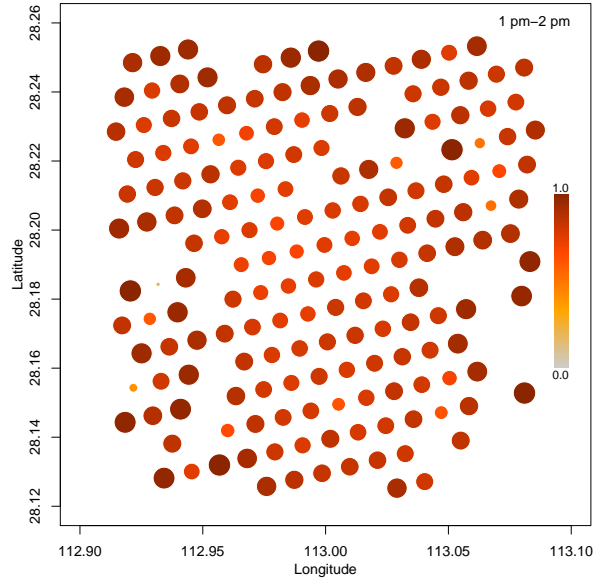


(d) Nighttime, Downwards

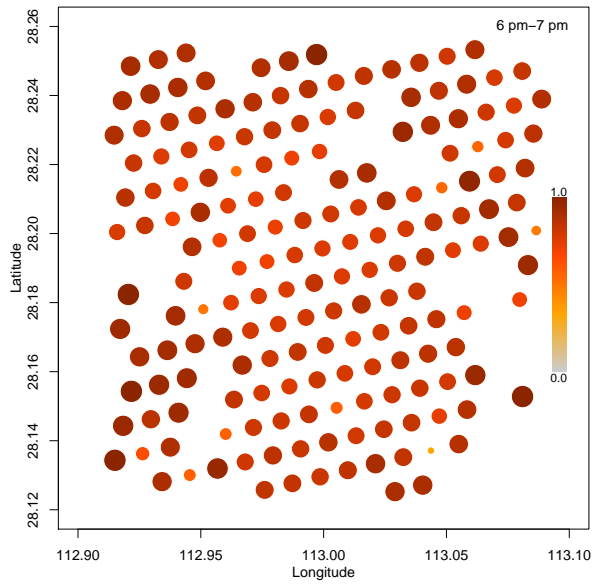
Figure 8: Choice probability of idle drivers on stepwise movements in zonal search during the a, b) daytime and c, d) nighttime. Compared to the daytime, idle drivers during the nighttime show a much higher tendency to move rather than stay motionless. Further, the pattern of drivers gathering from the suburban areas to the downtown is greatly strengthened at night. The upward(downward) arrows in the south(north) side carry darker colors compared to the north(south), which indicates drivers' inclination to move towards the central area.



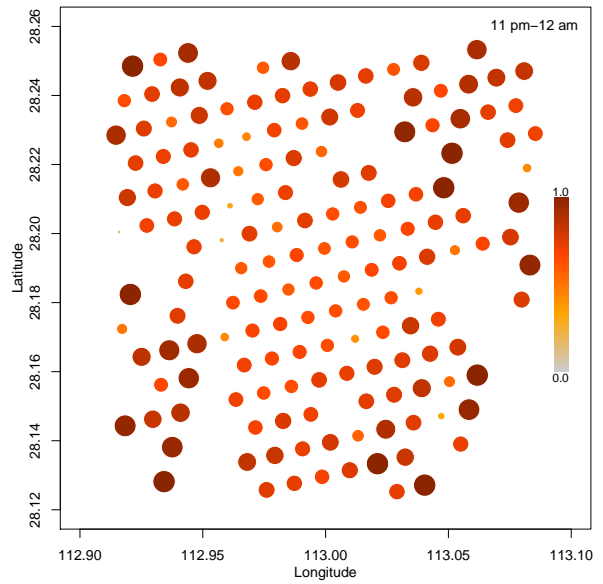
(a) Morning peak



(b) Midday

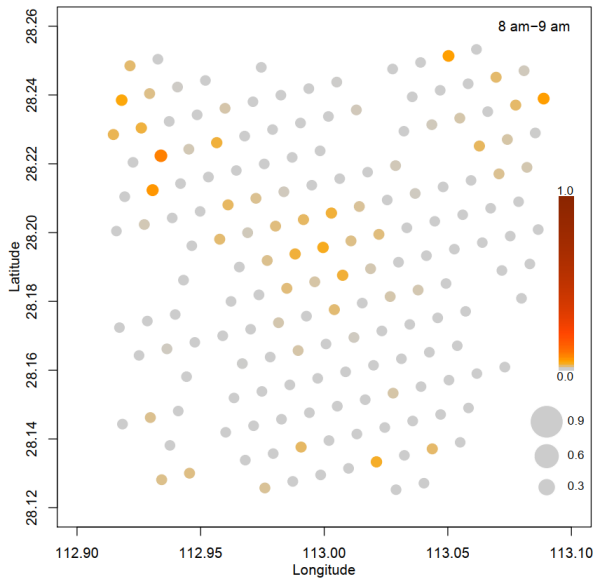


(c) Evening peak

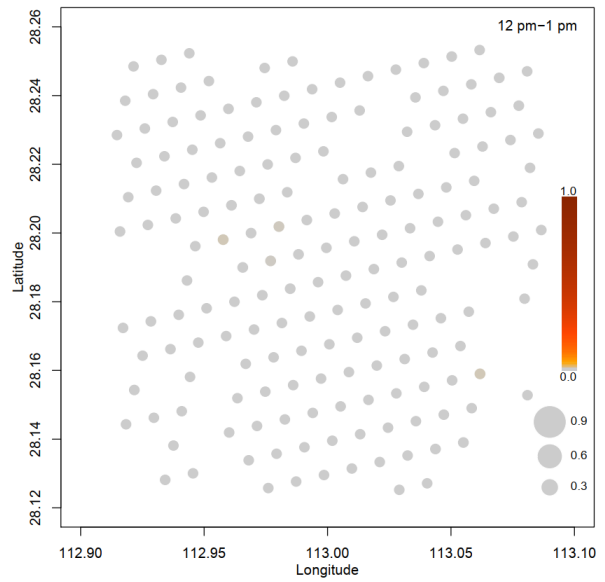


(d) Midnight

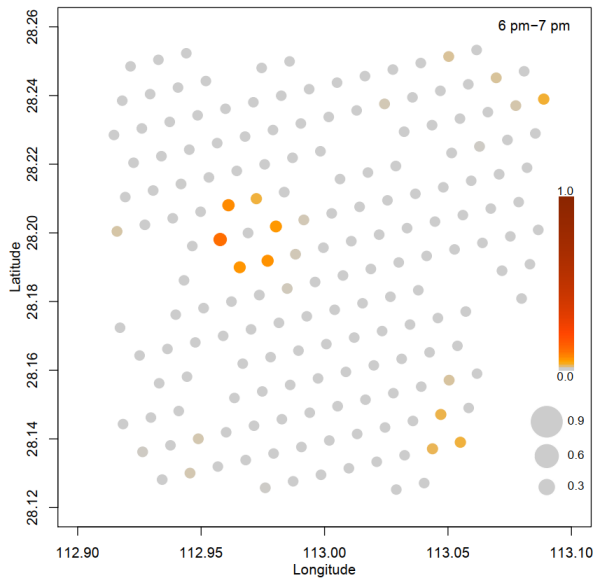
Figure 9: Choice probability of idle drivers staying motionless in each zone



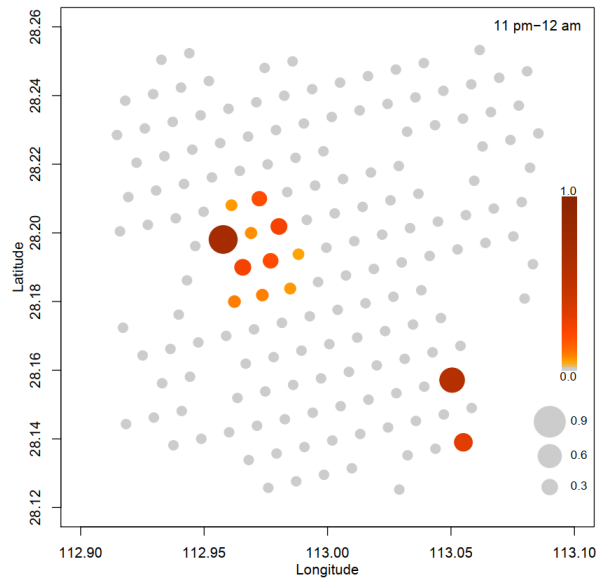
(a) Morning peak



(b) Midday



(c) Evening peak



(d) Midnight

Figure 10: Choice probability of idle drivers cruising nearby in each zone. Note that the three pies in the right corner carry the sizes corresponding to the probability levels of 0.3, 0.6, and 0.9 for reference.

442 supply and demand at different time and locations in the market. For the idle drivers at hotspots,
443 zigzagging in space may substantially lessen their matching time, given the relatively denser fleet
444 supply and thus more fierce competition there (see Figure 4a). But the same strategy could lead
445 to marginal improvements for ride-sourcing drivers in the cases with both demand and supply
446 being sparse in space. It would be worthwhile to empirically verify these hypotheses in the
447 future, to help reinforce the supply management of app-based ride-hailing services and yield
448 more desirable guidance for idle drivers.

449 5 Conclusion and discussion

450 To the best of our knowledge, this paper is among the first attempts to investigate ride-sourcing
451 drivers' customer-searching behavior. A dynamic discrete choice model has been proposed to
452 rationalize the time-dependent search movements of idle drivers within the spatial market. The
453 proposed model enables us to evaluate the impacts of spatiotemporal market conditions and un-
454 derstand the searching behavior of different classes of drivers. In particular, our model considers
455 the unobservable intentions behind drivers' searching movements. Based on two large-scale
456 datasets from real-world operations, we calibrate drivers' context-aware sensitivity to various
457 factors in their decision-making when idle. Statistical testing results confirm that there exists
458 a significant disparity between full-time and part-time drivers, and drivers' preferences in cus-
459 tomer search vary across time and space. The supply management of ride-sourcing platforms
460 could be further enhanced by accounting for these differentiated preferences of drivers:

- 461 • In general, ride-sourcing drivers respond actively to the repetitive market variations, with
462 full-time drivers being more sensitive and far-sighted compared to part-time drivers. Plat-
463 forms could thus customize searching guidance by accenting opportunities in nearby and
464 broader spaces for part-time and full-time drivers, respectively.
- 465 • Catering better to drivers' time-dependent appetites, ride-hailing platforms need to vary
466 the strategies for supply management. Drivers in idle prefer to stay motionless during
467 the daytime but become significantly more mobile late at night actively seeking matching
468 opportunities. Correspondingly, monetary incentives can be essential in stimulating idle
469 drivers to reposition favorably in the day, while sharing information that helps reduce their
470 idle time may be more welcomed when the market cools down at night.
- 471 • Drivers' aversion to the moving cost gives rise to their profound propensity to stay mo-
472 tionless when idle, especially in the suburbs where matching opportunities are scarce. It is
473 thus difficult and costly to reposition idle drivers out of those less demanded areas. Once
474 ended up there, drivers may be trapped with a long time of idleness. Such weak "self-
475 adjustments" of idle drivers stress the importance of demand rationing for supply manage-
476 ment. As customer trips deeply shape the supply availability in space, strategic pricing and
477 matching that account for riders' destinations are critical for efficient circulation of supply
478 resources.
- 479 • Customer-searching movements of drivers are not confined to local considerations. Instead,
480 they show a clear tendency of repositioning towards faraway targets, and such inclination
481 rises significantly as they stay closer to hotspot areas. As a result, compared to coldspots
482 and hotspots, the supply at the middle ground can be relatively unsustainable. It may be
483 drained up by hotspots, causing deceptive supply shortages. Hence, the platform may need

484 to pay more attention to the areas surrounding hotspots to prevent overwhelmed supply
485 rebalancing.

- 486 • On the whole, ride-sourcing drivers in the city do not cruise vigorously in local, as online
487 matching overcomes the physical obstacles in customer search. Cruising behavior only gets
488 intense isolatedly in the evening near the downtown and the railway station, where drivers
489 strive to win over other competitors by moving inches closer to potential riders. The intense
490 cruising in those few circumstances essentially signifies the mismatch of overall supply
491 and demand therein. Appropriately, platforms should discourage drivers from dwelling
492 in those oversupplied areas or adopt more transparent matching mechanisms to ease the
493 fruitless competition.

494 The outcomes of this study suggest that multifaceted concerns/attitudes of drivers, other
495 than regular market factors, can significantly dictate their customer-searching behavior. All these
496 complexities and uncertainties of drivers in idle/searching movements pose challenges to the
497 system operations. Therefore, to improve the supply management in the market, some ride-
498 sourcing platforms have started recruiting contracted drivers, who are required to follow the
499 platform's matching and repositioning instructions and paid with fixed income (Dong et al.,
500 2020). One of the promising future topics is thus to investigate how to effectively utilize such a
501 group of contractors and turn them into system actuators/controllers. Differentiated matching
502 and repositioning of contractors could be effective in addressing the spatial imbalance of supply
503 and demand, and substantially improve the efficiency of a ride-hailing system (Yang et al., 2020).

504 **Acknowledgements**

505 We would like to thank Dr. Pinghua Gong's team at Didi Chuxing for their professional and
506 invaluable assistance in data access for this empirical research. The work described in this pa-
507 per was partly supported by research grants from the US National Science Foundation (CMMI-
508 1854684; CMMI-1904575), the Hong Kong Research Grants Council (No. HKUST16208619), the
509 NSFC/RGC Joint Research Scheme under project N_HKUST627/18 (NSFC-RGC 71861167001),
510 and Didi Chuxing.

511 **References**

- 512 Conway, M. W., Salon, D., and King, D. A. (2018). Trends in taxi use and the advent of ridehailing,
513 1995–2017: Evidence from the us national household travel survey. *Urban Science*, 2(3):79.
- 514 Daly, A. and Bierlaire, M. (2006). A general and operational representation of generalised extreme
515 value models. *Transportation Research Part B: Methodological*, 40(4):285–305.
- 516 Dong, T., Xu, Z., Luo, Q., Yin, Y., Wang, J., and Ye, J. (2020). Optimal contract design for
517 ride-sourcing services under dual sourcing. Available at SSRN: [https://ssrn.com/abstract=](https://ssrn.com/abstract=3658335)
518 3658335. Accessed on August 9, 2020.
- 519 Fosgerau, M., Frejinger, E., and Karlstrom, A. (2013). A link based network route choice model
520 with unrestricted choice set. *Transportation Research Part B: Methodological*, 56:70–80.

- 521 Gao, Y., Jiang, D., and Xu, Y. (2018). Optimize taxi driving strategies based on reinforcement
522 learning. *International Journal of Geographical Information Science*, 32(8):1677–1696.
- 523 Lin, K., Zhao, R., Xu, Z., and Zhou, J. (2018). Efficient large-scale fleet management via multi-
524 agent deep reinforcement learning. In *Proceedings of the 24th ACM SIGKDD International Con-
525 ference on Knowledge Discovery & Data Mining*, pages 1774–1783.
- 526 Liu, S., Araujo, M., Brunskill, E., Rossetti, R., Barros, J., and Krishnan, R. (2013). Understand-
527 ing sequential decisions via inverse reinforcement learning. In *2013 IEEE 14th International
528 Conference on Mobile Data Management*, volume 1, pages 177–186. IEEE.
- 529 Qu, M., Zhu, H., Liu, J., Liu, G., and Xiong, H. (2014). A cost-effective recommender system
530 for taxi drivers. In *Proceedings of the 20th ACM SIGKDD international conference on Knowledge
531 discovery and data mining*, pages 45–54.
- 532 Rong, H., Zhou, X., Yang, C., Shafiq, Z., and Liu, A. (2016). The rich and the poor: A markov
533 decision process approach to optimizing taxi driver revenue efficiency. In *Proceedings of the 25th
534 ACM International on Conference on Information and Knowledge Management*, pages 2329–2334.
- 535 Rust, J. (1987). Optimal replacement of gmc bus engines: An empirical model of harold zurcher.
536 *Econometrica: Journal of the Econometric Society*, pages 999–1033.
- 537 Rust, J. (2016). *Dynamic Programming*, pages 1–26. Palgrave Macmillan UK, London.
- 538 Sahr, K., White, D., and Kimerling, A. J. (2003). Geodesic discrete global grid systems. *Cartography
539 and Geographic Information Science*, 30(2):121–134.
- 540 Shou, Z., Di, X., Ye, J., Zhu, H., Zhang, H., and Hampshire, R. (2020). Optimal passenger-
541 seeking policies on e-hailing platforms using markov decision process and imitation learning.
542 *Transportation Research Part C: Emerging Technologies*, 111:91–113.
- 543 Sun, H., Wang, H., and Wan, Z. (2019). Model and analysis of labor supply for ride-sharing
544 platforms in the presence of sample self-selection and endogeneity. *Transportation Research Part
545 B: Methodological*, 125:76–93.
- 546 Szeto, W., Wong, R., and Yang, W. (2019). Guiding vacant taxi drivers to demand locations
547 by taxi-calling signals: A sequential binary logistic regression modeling approach and policy
548 implications. *Transport Policy*, 76:100–110.
- 549 Tang, J., Wang, Y., Hao, W., Liu, F., Huang, H., and Wang, Y. (2019). A mixed path size logit-
550 based taxi customer-search model considering spatio-temporal factors in route choice. *IEEE
551 Transactions on Intelligent Transportation Systems*.
- 552 Train, K. E. (2009). *Discrete choice methods with simulation*. Cambridge university press.
- 553 Verma, T., Varakantham, P., Kraus, S., and Lau, H. C. (2017). Augmenting decisions of taxi
554 drivers through reinforcement learning for improving revenues. In *Twenty-Seventh International
555 Conference on Automated Planning and Scheduling*.
- 556 Wang, H. and Yang, H. (2019). Ridesourcing systems: A framework and review. *Transportation
557 Research Part B: Methodological*, 129:122–155.
- 558 Watson, P. L. and Westin, R. B. (1975). Transferability of disaggregate mode choice models.
559 *Regional Science and Urban Economics*, 5(2):227–249.

- 560 Wong, R., Szeto, W., and Wong, S. (2014a). Bi-level decisions of vacant taxi drivers traveling to-
561 wards taxi stands in customer-search: Modeling methodology and policy implications. *Trans-*
562 *port Policy*, 33:73–81.
- 563 Wong, R., Szeto, W., and Wong, S. (2014b). A cell-based logit-opportunity taxi customer-search
564 model. *Transportation Research Part C: Emerging Technologies*, 48:84–96.
- 565 Wong, R. C., Szeto, W., and Wong, S. (2015). Sequential logit approach to modeling the customer-
566 search decisions of taxi drivers. *Asian Transport Studies*, 3(4):398–415.
- 567 Xu, Z., AMC Vignon, D., Yin, Y., and Ye, J. (2020). An empirical study of the labor supply of
568 ride-sourcing drivers. *Transportation Letters*, pages 1–4.
- 569 Yang, K., Tsao, M. W., Xu, X., and Pavone, M. (2020). Planning and operations of mixed fleets in
570 mobility-on-demand systems. Available at arXiv: <https://arxiv.org/pdf/2008.08131.pdf>.
571 Accessed on December 10, 2020.
- 572 Yu, J. J., Tang, C. S., Max Shen, Z.-J., and Chen, X. M. (2020). A balancing act of regulating
573 on-demand ride services. *Management Science*, 66(7):2975–2992.
- 574 Zhang, D., Sun, L., Li, B., Chen, C., Pan, G., Li, S., and Wu, Z. (2014). Understanding taxi
575 service strategies from taxi gps traces. *IEEE Transactions on Intelligent Transportation Systems*,
576 16(1):123–135.
- 577 Zheng, Z., Rasouli, S., and Timmermans, H. (2018). Modeling taxi driver anticipatory behavior.
578 *Computers, Environment and Urban Systems*, 69:133–141.